12C states populated in 10B+10B reactions

Jelavić Malenica, Deša; Milin, Matko; Blagus, Saša; Di Pietro, A.; Figuera, P.; Lattuada, M.; Miljanić, Đuro; Musumarra, M.; Pellegriti, M.G.; Prepolec, Lovro; ...

Source / Izvornik: **Physical Review C, 2019, 99**

Journal article, Published version
Rad u časopisu, Objavljena verzija rada (izdavačev PDF)

https://doi.org/10.1103/PhysRevC.99.064318

Permanent link / Trajna poveznica: https://urn.nsk.hr/urn:nbn:hr:217:072276

^{12}C states populated in ^{10}B + ^{10}B reactions

D. Jelavić Malenica,[1,*] M. Milin,[2,†] S. Blagus,[1] A. Di Pietro,[3] P. Figuera,[3] M. Lattuada,[3] Đ. Miljanić,[1] A. Musumarra,[3] M. G. Pellegriti,[3] L. Prepolec,[1] V. Scuderi,[3] N. Skukan,[1] N. Soić,[1] S. Szilner,[1] D. Torresi,[3] and M. Uroić[1]

[1]*Division of Experimental Physics, Ruđer Bošković Institute, HR-10000 Zagreb, Croatia*

[2]*Physics Department, Faculty of Science, University of Zagreb, HR-10000 Zagreb, Croatia*

[3]*INFN - Laboratori Nazionali del Sud and Sezione di Catania, I-95123 Catania, Italy*

(Received 21 July 2017; revised manuscript received 9 May 2019; published 17 June 2019)

^{10}B + ^{10}B reactions are measured with 50 and 72 MeV beams. The large spin of both beam and target nuclei ($J^\pi = 3^+$) is particularly suitable for the population of high spin states in the exit channels. Population and decay of different states in ^{12}C are studied through sequential decay reactions. The ^{12}C excitation energy spectrum obtained from the ^{10}B(^{10}B, ^{8}Be) reaction shows a number of both known and new states. In particular, a new state at $E_x = 24.4$ MeV is observed to be strongly populated in the triple α-particle coincidences. The rarely seen state at $E_x = 30.3$ MeV is found to be strong in the d + ^{10}B decay channel, reinforcing the previous suggestions that it has the exotic $2\alpha + 2d$ molecular structure.

DOI: 10.1103/PhysRevC.99.064318

I. INTRODUCTION

Not many nuclei are so thoroughly studied (both experimentally and theoretically) as ^{12}C, a seemingly simple quantum system of only six protons and six neutrons. A large part of that interest arise from its importance in stellar nucleosynthesis: it is essential for the helium burning phase and, as such, it is crucial for production of all heavier elements. But a significant part of the interest stems also from purely fundamental motives to understand the ^{12}C structure in its full complex richness from basic principles.

A special status among the ^{12}C states is reserved to the second 0^+ state, at $E_x = 7.65$ MeV. This so-called Hoyle state [1] is within the Gamow window above the α-decay threshold (7.37 MeV) and, as such, it is responsible for the dramatic speed-up of helium burning [2]. Among all excited states in all nuclei, this makes the Hoyle state the single most important one (for nucleosynthesis), because most of the nuclei heavier than carbon are virtually produced through it.

Modeling the Hoyle state turned out to be a non-trivial task because it seems to have a unique structure [2], different even from the neighboring light nuclei which are often unusual themselves. Identifying the ^{12}C states related (as, e.g., rotational excitations) to the Hoyle state could help that mission, as well as completing and systematizing the ^{12}C spectroscopy in general. An important step in that direction was a recent work [3] reporting a new state (5^- at $E_x = 22.4$ MeV), and explaining most of the low-lying ^{12}C states as corresponding to a triangular oblate spinning top with a $\mathcal{D}_{3h}$ symmetry [4].

The ^{12}C structure is also discussed within the frameworks of many other theoretical models, starting with classic cluster microscopic 3α-cluster models such as the resonating group method (RGM), generator coordinate method (GCM), and orthogonality condition method (OCM) [5–12], including the more recent ones based on antisymmetrized molecular dynamics (AMD) [13], fermionic molecular dynamics [14], or the ones describing some ^{12}C states as Bose-Einstein condensates [15–17], and finally recent *ab initio* no-core shell model calculations [18], the no-core symplectic model [19], and effective field theory calculations on the lattice [20,21]. The obviously unusual structure of the Hoyle state is also reflected by the fact that it cannot be simply described within shell model calculations, even when $4\hbar\omega$ excitations are included [22]. A very recent review of microscopic clustering in nuclei [23] gives more details on theoretical progress made in explaining the ^{12}C structure (as well as many other nuclei).

From the experimental side, ^{12}C is still the focus of many new measurements. In the already mentioned recent experimental work by Lámbarri *et al.* [3] a new state was found at $E_x = 22.4(2)$ MeV using inelastic excitation of the ^{12}C target nuclei by an α-particle beam and sequential decay of ^{12}C into the 3α channel. The state was suggested to have $J^\pi = 5^-$ and to fit very well to the predicted ground state rotational band of an oblate equilateral triangular spinning top with $\mathcal{D}_{3h}$ symmetry. These results are consistent with the findings of several other measurements [24–27], that were focused on studies of the Hoyle state and its possible excitations. A new state is also found [28] at $E_x = 13.3$ MeV and assigned $J^\pi = 4^+$. The detection efficiency in most of the mentioned experiments fell strongly above ≈20 MeV, so higher lying states (discussed in this paper) were not seen.

Most of the ^{12}C states below $E_x \approx 20$ MeV fit [3] into the spectrum predicted by modeling ^{12}C as triangular oblate spinning top with $\mathcal{D}_{3h}$ symmetry [4]. However, that and other models predict also a number of states at higher excitation energies, e.g., AMD calculations [13] predict 2^+, 3^-, 5^-, and 6^+ states within 10 MeV from the 3α threshold, and those were not yet identified. It is important to identify excited

*desa.jelavic@irb.hr

†matko.milin@phy.hr

negative parity states (3^-, 4^-) associated with the Hoyle state, in order to distinguish between its different geometric interpretations; there are also predictions that these states will not be seen at all [29].

Completing the experimental data for ^{12}C is therefore essential, also at higher excitation energies. A recent study [30] of the high excitation energy region ($E_x > 15$ MeV) using the ^{12}C(^{3}He, ^{3}He)3α reaction found states at 16.3 (0.2), 17.2 (0.2), 18.4 (0.2), 19.7 (0.2), 22.2 (0.3), and 25.1 (0.3) MeV. Some of these states can be related to states already listed in the last compilation [31], while at least some of them are new states. The results support the earlier assignment of the 22.4 MeV state (in that experiment [30] seen at $E_x =$ 22.2 MeV) as the 5^- member of the rotational band of an oblate equilateral triangular spinning top with $\mathcal{D}_{3h}$ symmetry. Some suggestions are also given regarding the structure of the 19.7 and 25.1 MeV states, but further experimental results are needed (e.g., spins and branching ratios for the decay to the ^{8}Be$_{2^+} + \alpha$ channel).

The present paper reports on results concerning several ^{12}C states populated through ^{10}B + ^{10}B reactions. The complex structure of the low-lying states of the ^{10}B nucleus, which can be described as a mixture of shell model and cluster configurations of the type ^{6}Li$_{gs} + \alpha$ or ^{6}Li$(0_2^+, 1) + \alpha$, together with a high spin of the ground state $J^\pi = 3^+$, are expected to enable the population of a range of different high-spin states in a variety of nuclei around $A \approx 10$, at high excitation energies. In this work we give only results for the ^{12}C states populated through different exit channels, while data obtained for cluster states of several other isotopes (^{10,11}B, ^{11}C, ^{14}N, etc.) will be given in a followup paper. In the next sections we first give details of the performed experiment and the obtained experimental results, which is then followed by a discussion of the observed ^{12}C states.

II. EXPERIMENT

In order to further study the structure of nuclei in the $A \approx 10$ mass region, the ^{10}B + ^{10}B reactions were measured at beam energies of 50.0 and 72.2 MeV. The experiment was performed at INFN-LNS Catania, using the SMP Tandem accelerator and targets enriched in ^{10}B up to 99.8%. Reaction products were detected with a highly segmented detector setup covering a large solid angle and allowing the detection of single events as well as two- and three-particle coincidences. The selectivity of the ^{10}B + ^{10}B reactions in populating different states of neighboring nuclei was studied, together with the sequential decay of states in question. Data were collected in the coincidence mode.

The detector setup consisted of four ΔE-E silicon telescopes, each composed of a thin ΔE detector (57–67 μm), divided into four quadrants and a thick double-sided silicon strip detector (DSSSD) (500 or 1000 μm), divided into 16 strips in both front and back sides. Three detector setups were used, with different polar angles of the detector centers: setup 1 (40°, 20°, −20°, −40°), setup 2 (40°, 20°, −30°, −50°), and setup 3 (46°, 26°, −33°, −53°). Each detector covered polar angles in the range ±4° around the center, with openings in the azimuthal angles corresponding to the distance to the target equal to ≈36 cm. Different setups were better optimized for different reaction exit channels and excitation energies of the reaction products, and results from all three were combined to get a whole picture.

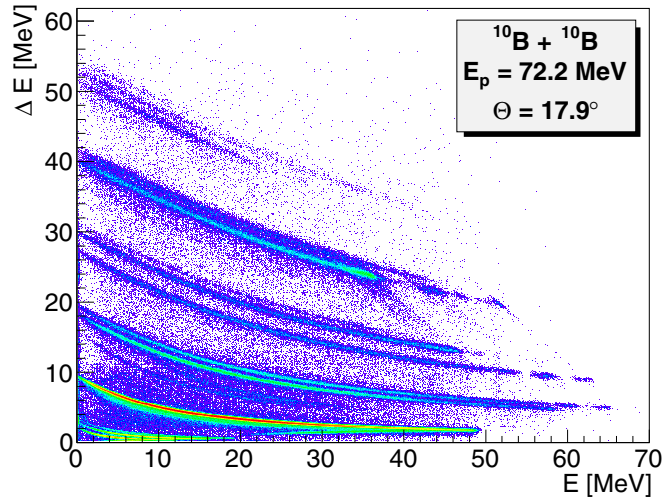

FIG. 1. An example of the ΔE-E spectrum for one quadrant of the thin detector and corresponding strips of the DSSSD thick detector in the telescope centered at 20° (see text for details).

Due to the large size of all detectors (50 × 50 mm^2) and their segmentation, telescopes covered a rather broad solid angle with good angular resolution. This same segmentation makes the analysis of obtained experimental data rather demanding; complications associated with dead layers [32] or interstrip gaps [33,34] are only part of the problem, the very basic one being a calibration of a large number of apparently independent detector channels. Several novel procedure improvements [35] allowing easy and accurate calibration of DSSSDs were used in the analysis; further procedures and details can be found in Ref. [36].

At both beam energies (50 and 72 MeV) the number of detected α particles was remarkably higher than the number of any other detected nuclei. This effect was more pronounced in coincident events, where even triple α-particle coincidences were detected with rather large statistics. Figure 1 gives an example of the ΔE-E spectrum for one quadrant of the telescope on angle 17.9°, where different particles can be seen, from protons, via the most abundant ^{4}He, up to ^{13}C, which was the heaviest particle detected. High-energy instances of the lightest detected particles (hydrogen and helium isotopes) passed through the detectors and therefore were excluded from the analysis (those events are anyway irrelevant for the results presented here). Several loci (in between helium and lithium ones) correspond to the pileup in a quadrant of the ΔE component of different telescopes; those events were also clearly separated and rejected from the subsequent analysis.

III. RESULTS

A. The ^{10}B(^{10}B, $\alpha\alpha$) reaction

If in the reaction channel ^{10}B(^{10}B, $\alpha\alpha$) two α particles are detected in coincidence, by assuming the reaction to be

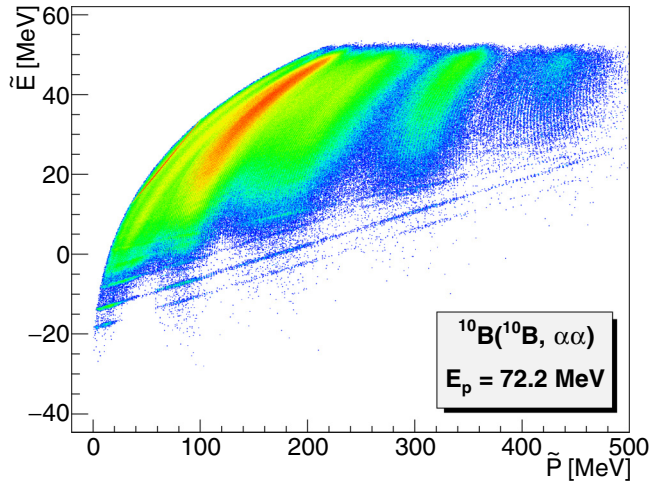

FIG. 2. Energy-momentum plot for α-α coincidences seen in all detector combinations, with all three setups included.

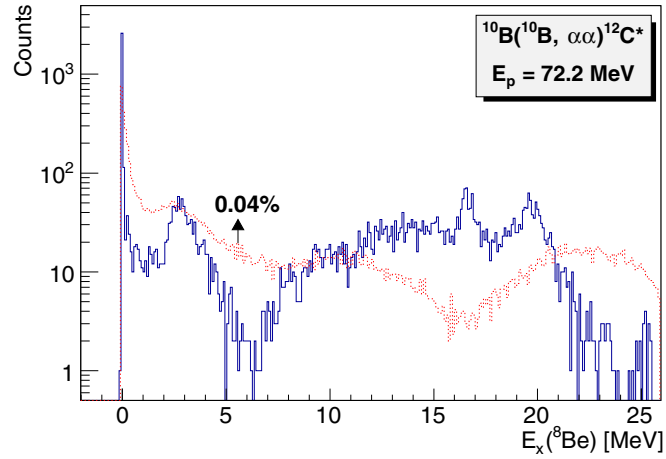

FIG. 3. The ^{8}Be excitation energy spectrum for the α-α coincidences, with undetected ^{12}C left in its first excited state (2^+ at 4.44 MeV). Events seen for all detector combinations and all setups are included.

three-body, one can use conservation laws to evaluate energy and momentum (E_3, P_3) of the third undetected particle (i.e., ^{12}C). Using the procedure suggested by [37] to produce the plot shown in Fig. 2, where $\tilde{E} = E_3 - Q$ and $\tilde{P} = p_3^2/(2m)$, one can observe different lines having the same slope. These lines correspond to different Q values, with the undetected ^{12}C being left in different excited states (discussed later). Banding of the lines arises from the gaps in the detector acceptance with angle.

Figure 2 allows us to verify if the detected particles are coming from reaction on the ^{10}B nuclei. Reactions induced on the ^{12}C contamination in the target were also seen, but they have different slope and can be separated from the subsequent analysis. Most of the events in Fig. 2 (i.e., events at high values of $\tilde{E}$) correspond to the reactions in which ^{12}C is either highly excited or not produced at all as an intermediate particle.

Choosing events along one line of Fig. 2, one can study the $^{10}\mathrm{B} + ^{10}\mathrm{B} \rightarrow \alpha + \alpha + ^{12}\mathrm{C}^*$ reaction with (undetected) ^{12}C left in a given state. Assuming two detected α particles are coming from sequential decay of ^{8}Be, production of the ^{8}Be excitation energy spectrum is straightforward; one such spectrum (the one when ^{12}C is left in the first excited state at $E_x = 4.44$ MeV) is given in Fig. 3. Several ^{8}Be states are clearly seen: ground state (g.s.), 2^+ at $E_x = 3.03$ MeV, 2^+ at $E_x = 16.92$ MeV, and probably 4^+ at $E_x = 19.86$ MeV (our peak has a centroid at 19.9 MeV; there is also another nearby known state, 2^+ at $E_x = 20.1$ MeV). The 4^+ state at E_x= 11.35 MeV (the third member of the ground state rotational band) is probably also populated, but due to its very large width ($\Gamma \approx 3.5$ MeV) its shape in the spectrum is significantly modulated with the detection efficiency effects (the same is true, to a lesser extent, for the 3.03 MeV state). The listed states are, as expected, the strongest ^{8}Be states populated in other deuteron stripping reactions from ^{10}B, see, e.g., [38]. Sequential decay through the ^{16}O states is also contributing to the spectrum given in Fig. 3, but it is found to be rather weak.

Of course, the ^{8}Be excitation energy spectrum can also be produced for *all* events from Fig. 2, but since a large portion of them are not coming from sequential decay via ^{8}Be, the spectrum shows fewer peaks. Actually, the only peak visible aside from the very strong ^{8}Be ground state (note the logartihmic scale on the y axis of Fig. 3) is a peak at $E_x \approx 0.5$ MeV; it does not correspond to an actual ^{8}Be state, but is rather a signature (see, e.g., [39,40]) of the fact that two α particles are coming from a sequential decay of the 2.43 MeV state in ^{9}Be (results for ^{9}Be, ^{10}B, and some other nuclei will be discussed in a separate paper).

As seen in Fig. 3, the ^{8}Be ground state can be easily separated and corresponding events further analyzed. Choosing the events from Fig. 2 corresponding to two α particles coming from the ^{8}Be ground state, one can reconstruct the excitation energy spectrum of undetected ^{12}C, corresponding to the ^{10}B(^{10}B, ^{8}Be) reaction.

This is shown in the inset of Fig. 4, while the main figure shows the spectrum with subtracted background. ^{12}C excited to high-lying states predominately decays into the three α particles, generating a total of five α particles in the exit channel. Therefore there are different contributions to the background of Fig. 4, but a simple polynomial (of the fourth order) seems to fit it well.

After background subtraction, several strong peaks (states in ^{12}C) can be easily identified in Fig. 4: g.s., 2^+ state at 4.44 MeV, 3^- at 9.64 MeV, and 5^- at 22.4 MeV (as proposed in [3]). The population of the g.s. is suppressed due to the large Q-value mismatch ($Q = 19.25$ MeV, $Q_{\mathrm{opt}} \approx -12$ MeV). A smaller but visible peak corresponds also to the known ^{12}C state at 7.65 MeV (Hoyle state). One can also see the unresolved overlapping group of states at E_x = 13–14 MeV, as well as peaks at E_x = 16.1, 19.8, 24.3, 27.4, and 30.3 MeV. The procedure can be repeated for the other ^{8}Be states; the population of more or less the same ones (with slightly different relative intensities) can be seen in all the obtained spectra, with the high energy part of the spectrum always dominated by the states at 22.4 and 30.3 MeV.

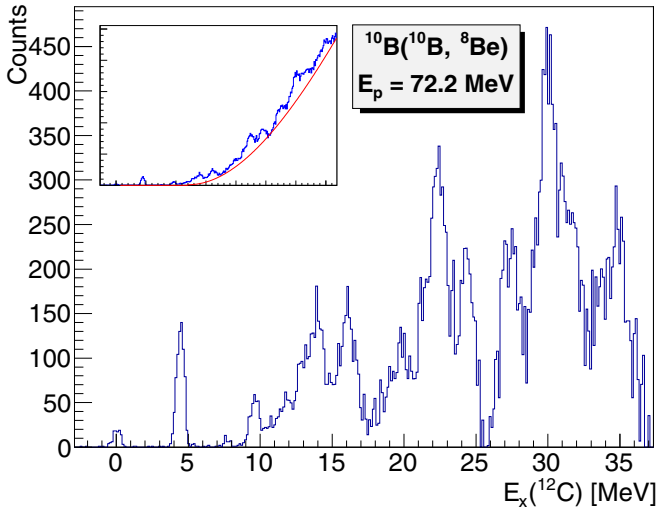

FIG. 4. The ^{12}C excitation energy spectrum for the 2α coincidences, obtained for events from Fig. 2, with an additional cut that two detected α particles are coming from the ^{8}Be ground state, and with subtracted background (the inset shows the spectrum with background).

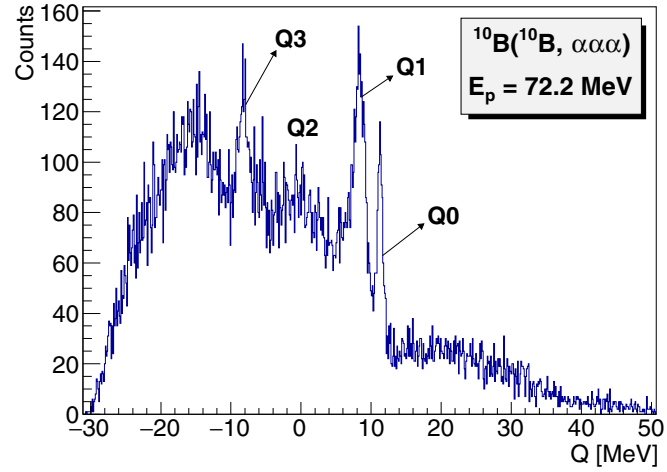

FIG. 5. The Q spectrum for the ^{10}B(^{10}B, 3α) reaction. Two of the three detected α particles are coming from the ^{8}Be(g.s.); see text for the details. All three detector setups were used.

Although very partial, angular distributions for the events given in Fig. 4 are very forward peaked, suggesting that the corresponding reaction mechanism is deuteron transfer; all the populated states have therefore non-negligible $^{10}\mathrm{B} + d$ strength. This point will be further discussed in the next sections.

B. The ^{10}B(^{10}B, 3α) reaction

Due to the large solid angle and high segmentation of the detector setup, α particles were detected (with large statistics) not only in double, but also in triple coincidences. If they are coming from the $^{10}\mathrm{B} + {}^{10}\mathrm{B}$ reactions, than the undetected part of the exit channel corresponds to the ^{8}Be nucleus, which is particle unstable, and decays exclusively [for $E_x(^{8}\mathrm{Be})$ up to $\approx$17.3 MeV] through the $\alpha + \alpha$ channel. By detecting three α particles in coincidence one can thus systematically probe the $^{10}\mathrm{B} + {}^{10}\mathrm{B} \rightarrow 5\alpha$ reaction and its different sequential paths. The first step of the procedure is to check if two of the α particles are coming from the ^{8}Be g.s. decay (with an energy of only 92 keV this decay has a clear signature in the detectors and is easily recognized and extracted). Once two such α particles are found, one can reconstruct the energy and angle of the ^{8}Be g.s. before decay and combine it with the third α particle, in search of possible ^{12}C states that are produced in the sequential decay to the 5α exit channel.

Figure 5 gives the Q spectrum for the ^{10}B(^{10}B, 3α) reaction, with three α particles detected in different detector combinations. All of the events in the figure proceed sequentially via the ^{8}Be ground state (the efficiency for detecting other states with the present detector setup is much smaller), so the first step in producing it is recognizing which two of the three detected α particles are coming from this ^{8}Be decay. After that ^{8}Be is treated as one particle, and a third α particle is added [37] to produce the Q-value (or missing mass) spectrum. Different peaks in Fig. 5 correspond to the excitations of the remaining (undetected) system, which is in this case again ^{8}Be (left in ground or different excited states).

In Fig. 5 obtained in that way, one can clearly see the population of the ground state of ^{8}Be (peak marked with "Q0"), the broad first excited state at $E_x(^{8}\mathrm{Be}) = 3.03$ MeV (Q1), the even broader second excited state at 11.35 MeV (Q2), and a narrow state at $\approx$19.9 MeV (Q3). These are, of course, the same states seen through the ^{10}B(^{10}B, $\alpha\alpha$)^{12}C reaction discussed previously (Fig. 3); only the state at 16.9 MeV in Fig. 3 is not that clearly seen in the present case. The background events (including those having $Q > 12$ MeV) in Fig. 5 correspond to the situation in which third detected α particle (i.e., the one *not* combined in the ^{8}Be g.s.) is not coming from the ^{12}C decay together with the reconstructed ^{8}Be, but is produced by some other process. By choosing one of the marked peaks in the Fig. 5, one can now probe the $^{12}\mathrm{C} \rightarrow 3\alpha$ decay; the background for peaks Q2 and Q3 is rather large, but Q0 and Q1 can be relatively easily extracted (even better with help from an energy-momentum plot similar to Fig. 2) and further discussed.

Choosing, e.g., the events from the Q1 peak (having better statistics than the Q0 peak), one can thus study the $^{10}\mathrm{B} + {}^{10}\mathrm{B} \rightarrow {}^{8}\mathrm{Be} + \alpha + {}^{8}\mathrm{Be}^{*}$ reaction. The final three-body exit channel can be reached through different two-body intermediate steps, which has to be checked by plotting relative energies (or the corresponding excitation energies) for all three possible pairs (i.e., effectively Dalitz plots). An example of such a plot is given in Fig. 6. The fact that horizontal lines are not seen in the plot suggests that the population of the ^{16}O intermediate states is weak or not present at all for this exit channel. Weak diagonal lines present in the spectrum are also due to the decay of the ^{12}C, but the one in which the α particle has to be combined with the other ^{8}Be nucleus in the exit channel.

Once that contribution from the ^{16}O intermediate states is dismissed, one can assume that most of the events are coming from the $^{10}\mathrm{B} + {}^{10}\mathrm{B} \rightarrow {}^{8}\mathrm{Be} + {}^{12}\mathrm{C}$ reaction and plot

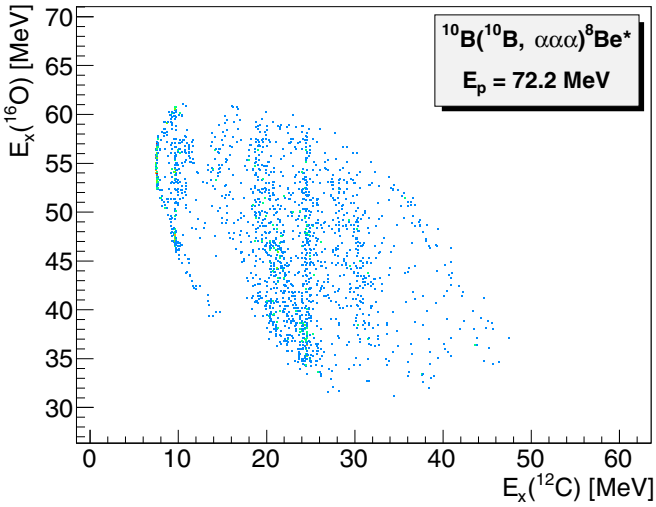

FIG. 6. Dalitz plot showing the reconstructed excitation energy of ^{16}O plotted against that of ^{12}C, for the events from the peak marked with Q1 in Fig. 5.

the corresponding ^{12}C excitation energy. Figure 7 gives the ^{12}C excitation energy spectrum reconstructed from the triple α-particle coincidences, with two of them being in the ^{8}Be ground state (and choosing two undetected α particles coming from the ^{8}Be first excited state, peak Q1 in Fig. 5). Figure 7 is obtained by summing spectra for different detector combinations; all individual ones are rather similar to each other, with the most important difference between them coming from different detection efficiency dependence on excitation energy (which is the consequence of geometry issues).

The detection efficiencies for given setups were obtained from a Monte Carlo (MC) code that simulated a two-body ^{10}B + ^{10}B reaction, assuming an isotropic c.m. distribution of products, followed by sequential decay into fragments,

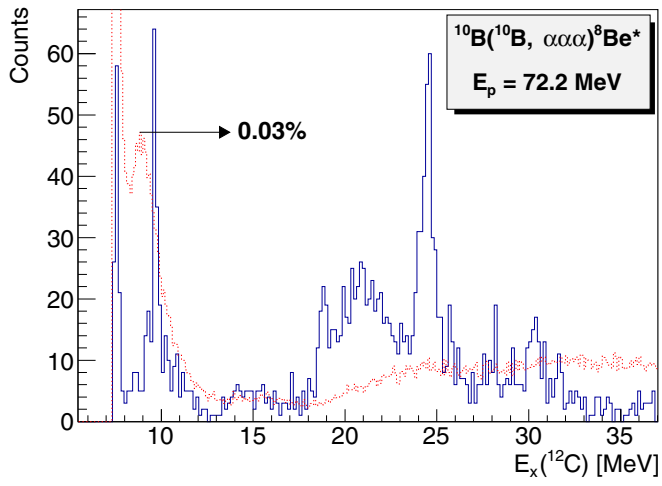

FIG. 7. The ^{12}C excitation energy spectrum for the 3α coincidences, for events from the Q1 peak in Fig. 5. All three setups are included together with all detector combinations, except the one where two α particles are detected in detector 3. The (red) dotted line shows the corresponding Monte Carlo efficiency curve.

assuming an isotropic c.m. distribution. The detection of the fragments was simulated both with angular cuts to mimic the solid angles covered by the telescopes and with energy cuts to simulate the detection thresholds of the telescopes. The efficiency curve (efficiency as a function of the excitation energy) obtained with the Monte Carlo simulation is given in Fig. 7 with a (red) dashed line; the absolute value of efficiency is given for a single point of the curve, so that it can be inferred for the rest of it.

The first peak in most efficiency curves (like the one in Fig. 7) comes from events where both particles are detected in the same telescope. The angle between the two particles then increases with increasing relative energy such that one of the particles misses the telescope in which the other particle is detected. The detection efficiency falls until particles have sufficient relative energy to hit two neighboring telescopes.

In most spectra for different combinations of detectors and all setups one can see contributions from the states at $E_x = 7.65$ and 9.64 MeV, so these are also clearly visible in the combined figure for all three setups (Fig. 7). The recently discovered state at $E_x = 22.4$ MeV [3] can also weakly be seen for some detector combinations, as well as some other states, but the dominant state at higher excitation (as clearly seen in Fig. 7) in most of the spectra is the state at $E_x =$ 24.4 MeV.

The composite spectrum given in Fig. 7 has an efficiency curve that shows some oscillations, which is the consequence of the fact that some particular combinations of detectors can have a rather narrow efficiency curve, contributing to the total one only in a small excitation energy range. To further confirm that the peak at $E_x = 24.4$ MeV is not an artificial one, produced by an increased detection efficiency in that excitation energy region, we have produced all the individual detector combinations. The detection efficiencies for those are always smooth and it is easy to recognize if some structure in the spectrum is only an experimental artifact. In a number of detector combinations, the peak is seen always at the same excitation energy ($E_x = 24.4$ MeV) and with the same width ($\Gamma = 0.50$ MeV), so it is without any doubt a genuine state in ^{12}C. The width of the peak corresponding to the 3^- state at $E_x = 9.64$ MeV in Fig. 7 is $\Gamma = 0.14$ MeV (its natural width is much smaller, 48 keV [41]), so this value can be considered as the experimental resolution in Fig. 7.

In Fig. 7 one can also see small peaks at 30.3 MeV (to be discussed in the next subsection), and at 18.4 MeV; the latter is not seen in the 2α coincidences (Fig. 4), but is reported in the recent measurement of the same ^{12}C excitation region by inelastic scattering of ^{3}He [30].

C. The ^{10}B(^{10}B, d^{10}B) reaction

Apart from the α-α pairs, a number of other particle combinations were measured in coincidence; a further combination relevant for the discussion of the ^{12}C nucleus is ^{10}B + d. Figure 8 gives the Q spectrum for the ^{10}B(^{10}B, d^{10}B) reaction; the obvious peak (marked as "Q0") corresponds to the third (undetected) particle (in this case ^{8}Be) left in its ground state. The events to the left of the peak correspond to either ^{8}Be or ^{10}B (or both) populated to their excited states; no single

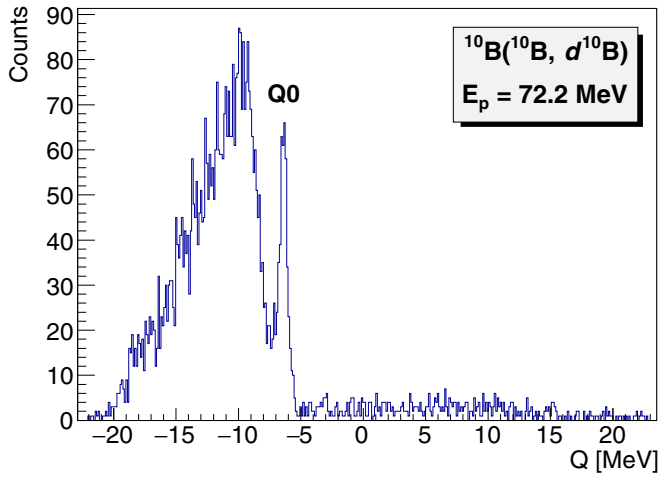

FIG. 8. The Q spectrum for the ^{10}B(^{10}B, d^{10}B) reaction, with all detector setups included, for particles detected in detectors 2 and 3.

peak could be resolved in this region. Gating on the Q0 peak, one can obtain the excitation energies in different two-body sub-systems (in this case ^{10}B, ^{12}C, and ^{18}F).

The energy-momentum plots show that intermediate states in ^{10}B are indeed populated in this channel, e.g., the one that is clearly seen is the 3^+ state ($T = 0$) at $E_x = 7.04$ MeV (the ^{10,11}B states populated in this experiment will be discussed in detail in a followup paper). The contributions from the ^{10}B intermediate states were easily rejected from further analysis because they corresponded to very narrow states. Sequential decay via the ^{18}F states were, on the other hand, not seen at all.

Figure 9 gives the ^{12}C excitation energy spectrum reconstructed from the $d + ^{10}$B coincidences. The state at $E_x = 30.3$ MeV is clearly visible, as was already seen through different reactions involving the ^{6}Li or ^{10}B nuclei (discussed later). The detection efficiency curve has a strong maximum at low energies (corresponding to two particles detected in the same telescope), while in the region of the peak it does not

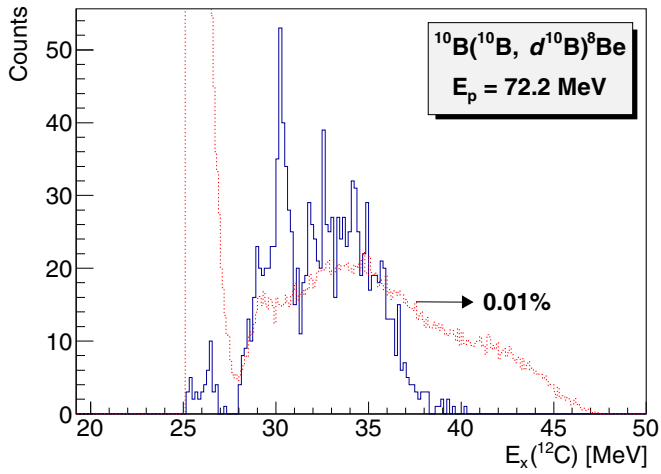

FIG. 9. The ^{12}C excitation energy spectrum for the $d + ^{10}$B coincidences, for Q state Q0, with all detector setups included. The (red) dotted line shows the corresponding Monte Carlo simulation.

have a pronounced structure. No other peaks are significantly populated in Fig. 9.

IV. DISCUSSION

A. The new state in ^{12}C at $E_x = 24.4$ MeV

Between 23.5 and 25.5 MeV of excitation energy, the last compilation for ^{12}C [31] lists seven states. Having $T = 1$, three of them were not populated in reactions studied here, and two of them have listed widths significantly larger than 1 MeV; the remaining two are the states at $E_x = 24.38$ MeV ($J^\pi = 2^+$, $\Gamma = 670$ keV) and state of unknown spin and parity at $E_x = 24.90$ MeV ($\Gamma = 920$ keV). Both states are seen as resonances in the ^{11}B$(p, n)^{11}$C excitation function, and are *not* seen at all to decay with α-particle emission. That fact, as well as rather different width, suggest that in Figs. 4 and 7 we do not see any of them, but rather a new state at $E_x = 24.4(2)$ MeV (with $\Gamma \approx 500 \pm 40$ keV), not yet listed in the compilation [31]. The uncertainty of the excitation energy and width of this state are estimated from the concurrence of our results with tabulated energies of the ^{12}C states at high excitation energies.

Although the complicated procedure used to produce Fig. 7 makes it impossible to precisely extract spin, parity, and partial decay widths of the new state, one can compare it to the other states populated in the same way. Its behavior in the obtained spectra seems to be the closest to the well known 3^- state at $E_x = 9.64$ MeV, shown to have a reduced α width, which indicates a clear cluster structure [41]. The cross section ratio for the two states in Fig. 4 is 6.6:1, while in Fig. 7, after correcting for different detection efficiencies, it is almost the same, 6.3:1. It should be noted that the detection efficiency is calculated (with Monte Carlo simulation) by assuming the isotropic decay of the populated ^{12}C states (i.e., neglecting their spins), so the last ratio is only approximately correct. Nevertheless, one can conclude that the 24.4 MeV state has a significant overlap with the ^{10}B + d and ^{8}Be + α configurations, as does the 9.64 MeV state. Both are also less pronounced in the Fig. 4 (i.e., deuteron transfer to ^{10}B) when compared to the other states with the $\mathcal{D}_{3h}$ symmetry: the 2^+ state at 4.44 MeV, 4^+ state at 14.08 MeV. and the recently proposed 5^- at 22.4 MeV.

On the other hand, when combined with the subsequent ^{8}Be + α decay, the states at 9.64 and 24.4 MeV become the strongest ones in the spectrum (Fig. 7), implying that their α-particle decay widths are significantly larger than the ones for the 14.08 and 22.4 MeV states (as is also seen for the 9.64 MeV state in Ref. [41]). Of course, the influence of the Coulomb and the centrifugal barriers is very different for the states at 9.64 and 24.4 MeV, and the discussion above must be regarded as only very schematic and qualitative.

All this may suggest that the state at 24.4 MeV has a structure that is closer to the Hoyle state than to the compact ^{12}C ground state. This is probably also a reason why this state is not seen in the recent precise measurements in which the ^{12}C states are populated with the inelastic scattering of ^{3}He or ^{4}He [3,30]. Of course, the spin and parity assignments for this new state are essential to find its place in the spectroscopy systematics of ^{12}C.

B. The ^{12}C state at $E_x = 30.3$ MeV

The state at $E_x = 30.3(2)$ MeV (with $\Gamma \approx 540 \pm 40$ keV) is clearly seen in Figs. 4 and 9; together with the 22.4 MeV states, it dominates the spectrum for the ^{10}B(^{10}B, ^{8}Be)^{12}C reaction (Fig. 4). In the spectrum showing the subsequent deuteron decay (Fig. 9), it is the only clearly populated state (the 22.4 MeV state is below the threshold for that decay).

The 30.3 MeV state has been seen in a number of previous experiments [31] giving results for the ^{10}B$(d, \alpha_0)^8$Be [42], ^{12}C$(\alpha, 4\alpha)$ [43], and ^{6}Li(^{6}Li, $\alpha_0)^8$Be [44] reactions. It is not reported in the recent measurements of inelastic scattering of α particles [3] or ^{3}He [30] because those were insensitive to such high excitation energies.

Although the state is dominating the spectra in Figs. 4 and 9, it is very weak (or not seen at all) in the spectra showing the sequential decay into three α particles (Fig. 7); that indicates that its structure involves degrees of freedom beyond the 3α configuration. It should also be noted that the width of the state turns out to be larger when extracted from the ^{10}B(^{10}B, d^{10}B) spectrum ($\Gamma \approx 830$ keV) compared to the ^{10}B(^{10}B, ^{8}Be) one ($\Gamma \approx 540$ keV); this is probably consequence of the nontrivial subtraction of the background for the first reaction, though one cannot exclude the possibility that two overlapping levels are contributing to the peak in Fig. 4.

Relatively small width ($\Gamma \approx 540$ keV) at very high excitation energy (30.3 MeV) indicates that it is a rather special state, having structure that preserves it from being spread and mixed with the continuum. The analysis of the distribution of the events in the Dalitz diagram for the reaction ^{12}C$(\alpha, 4\alpha)$ [43] suggests it has spin and parity $J^\pi = 2^+$. Furthermore, the excitation energy of the state is rather close to several thresholds: ^{6}Li + ^{6}Li (28.2 MeV), ^{6}Li + $\alpha + d$ (29.7 MeV), and $\alpha + \alpha + d + d$ (30.4 MeV). All these suggest (in accordance with Ikeda's threshold rule) that it might have a rather exotic $2\alpha + 2d$ molecular structure, unlike any of the (known) lower lying states.

C. Other ^{12}C states

A number of other rarely seen or new states are also present in our excitation spectra. In Fig. 4 one can thus see, next to the well known states (g.s., 2^+ at 4.44 MeV, 3^- at 9.64 MeV, 2^- at 11.83 MeV, and 4^+ at 14.08 MeV), states not listed in the compilation [31], at $E_x = 16.05$ ($\Gamma \approx 620$ keV), 19.83 ($\Gamma \approx 450$ keV), and 22.38 MeV ($\Gamma \approx 800$ keV). Those may correspond to the levels reported in the inelastic scattering experiment [30] at $E_x = 16.3$ ($\Gamma < 600$ keV), 19.7 ($\Gamma < 600$ keV), and 22.2 MeV ($\Gamma < 700$ keV) respectively. The last one is proposed to be the 5^- member of the ground state rotational band of an oblate equilateral triangular spinning top with $\mathcal{D}_{3h}$ symmetry, while the structure of others has not been discussed yet.

The peaks at 16.11 and 20.5 MeV were previously also clearly seen through the ^{10}B(^{3}He, $p\alpha\alpha\alpha$) reaction [26], but treated there as the $T = 1$ states (in accordance with the compilation [31]), which is inconsistent with their population in the present measurement; of course, it is possible that the two experiments are not seeing the same states.

It is also worth noting that there is a a broad structure under several narrow peaks at $E_x \approx 14.0$ MeV. Recent results by Zimmerman *et al.* [27] found the 2^+ excitation of the Hoyle state with resonant parameters $E_x = 10.13(6)$ MeV and $\Gamma = 2.1(3)$ MeV; if the state has a rotational character, the 4^+ state should be around $E_x \approx 14$ MeV and have rather large width. A new state was recently found [28] at $E_x = 13.3$ MeV and assigned $J^\pi = 4^+$.

Finally, there is also another strong peak in Fig. 4 at $E_x = 27.49$ MeV, not reported yet in other measurements. It is worth noting that the 6^+ member of the g.s. rotational band (with 2^+ at 4.44 MeV and 4^+ at 14.08 MeV) is expected to be at $E_x = 28$–30 MeV, so this state is a valid candidate (since it is as strongly populated in the Fig. 4 as the other members of the band).

V. SUMMARY

The nuclei with $A = 10$–12 nucleons, even when they have small isospin, host a number of interesting configurations, e.g., the still puzzling Hoyle state and its excitations, or the extremely deformed "nuclear molecules" in ^{10}Be [39]. Such configurations were searched for by studying the ^{10}B + ^{10}B reactions: with its g.s. having $J^\pi = 3^+$, ^{10}B is expected to be a good projectile/target for population of high spin states through various transfer reactions.

In this paper we report on the population of several new and rarely seen states in ^{12}C. By far the most abundant final products in exit channels of reactions were α particles, so we were able to study α-α and α-α-α coincidences and to reconstruct the associated ^{12}C spectra of intermediate states involved in the process.

A new state is found at $E_x = 24.4$ MeV, showing properties that seem to indicate a rather pronounced α-cluster structure. The rarely seen state at $E_x = 30.3$ MeV is found to dominate the ^{10}B(^{10}B, d^{10}B) spectrum, indicating that it might have an exotic $2\alpha + 2d$ molecular structure, different from all the lower lying ^{12}C states. Several other states are observed, with limited information on their structure. Further studies of high excitation energy region in ^{12}C, with emphasis on spin and parity assignments, are needed to complete our understanding of this rich and intriguing quantum system.

ACKNOWLEDGMENTS

The authors are grateful to the LNS staff for the good-quality beam and targets. This work has been supported in part by the Croatian Science Foundation under Project No. 7194.

[1] F. Hoyle, Astrophy. J. Suppl. Ser. **1**, 121 (1954).
[2] M. Freer and H. O. U. Fynbo, Prog. Part. Nucl. Phys. **78**, 1 (2014).
[3] D. J. Marín-Lámbarri, R. Bijker, M. Freer, M. Gai, T. Kokalova, D. J. Parker, and C. Wheldon, Phys. Rev. Lett **113**, 012502 (2014).

[4] R. Bijker and F. Iachello, Ann. Phys. (Amsterdam) **298**, 334 (2002).

[5] Y. Fukushima and M. Kamimura, in *Proceedings of the International Conference on Nuclear Structure, Tokyo, 1977*, edited by T. Marumori, Suppl. J. Phys. Soc. Jpn. **44**, 225 (1978).

[6] M. Kamimura, Nucl. Phys. A **351**, 456 (1981).

[7] Y. Fujiwara *et al.*, Prog. Theor. Phys. Suppl. **68**, 29 (1980).

[8] H. Horiuchi, Prog. Theor. Phys. **51**, 1266 (1974).

[9] H. Horiuchi, Prog. Theor. Phys. **53**, 447 (1975).

[10] E. Uegaki, S. Okabe, Y. Abe, and H. Tanaka, Prog. Theor. Phys. **57**, 1262 (1977).

[11] E. Uegaki, Y. Abe, S. Okabe, and H. Tanaka, Prog. Theor. Phys. **59**, 1031 (1978).

[12] E. Uegaki, Y. Abe, S. Okabe, and H. Tanaka, Prog. Theor. Phys. **62**, 1621 (1979).

[13] Y. Kanada-En'yo, Prog. Theor. Phys. **117**, 655 (2007).

[14] M. Chernykh, H. Feldmeier, T. Neff, P. von Neumann-Cosel, and A. Richter, Phys. Rev. Lett. **98**, 032501 (2007).

[15] A. Tohsaki, H. Horiuchi, P. Schuck, and G. Röpke, Phys. Rev. Lett. **87**, 192501 (2001).

[16] Y. Funaki, A. Tohsaki, H. Horiuchi, P. Schuck, and G. Röpke, Phys. Rev. C **67**, 051306(R) (2003).

[17] A. Tohsaki, H. Horiuchi, P. Schuck, and G. Röpke, Rev. Mod. Phys. **89**, 011002 (2017).

[18] R. Roth, J. Langhammer, A. Calci, S. Binder, and P. Navratil, Phys. Rev. Lett. **107**, 072501 (2011).

[19] A. C. Dreyfuss, K. D. Launey, T. Dytrych, J. P. Draayer, and C. Bahri, Phys. Lett. B **727**, 511 (2013).

[20] E. Epelbaum, H. Krebs, D. Lee, and U.-G. Meißner, Phys. Rev. Lett. **106**, 192501 (2011).

[21] E. Epelbaum, H. Krebs, T. A. Lähde, D. Lee, and U.-G. Meißner, Phys. Rev. Lett. **109**, 252501 (2012).

[22] P. Navrátil, J. P. Vary, and B. R. Barrett, Phys. Rev. Lett. **84**, 5728 (2000).

[23] M. Freer, H. Horiuchi, Y. Kanada-En'yo, D. Lee, and U.-G. Meißner, Rev. Mod. Phys. **90**, 035004 (2018).

[24] O. S. Kirsebom, M. Alcorta, M. J. G. Borge, M. Cubero, C. A. Diget, R. Dominguez-Reyes, L. M. Fraile, B. R. Fulton, H. O. U. Fynbo, S. Hyldegaard, B. Jonson, M. Madurga, A. Muñoz Martin, T. Nilsson, G. Nyman, A. Perea, K. Riisager, and O. Tengblad, Phys. Rev. C **81**, 064313 (2010).

[25] W. R. Zimmerman, N. E. Destefano, M. Freer, M. Gai, and F. D. Smit, Phys. Rev. C **84**, 027304 (2011).

[26] M. Alcorta, M. J. G. Borge, M. Cubero, C. Aa. Diget, R. Domínguez-Reyes, L. M. Fraile, B. R. Fulton, H. O. U. Fynbo, D. Galaviz, S. Hyldegaard, H. Jeppesen, B. Jonson, O. S. Kirsebom, M. Madurga, A. Maira, A. Muñoz-Martín, T. Nilsson, G. Nyman, D. Obradors, A. Perea, K. Riisager, O. Tengblad, and M. Turrion, Phys. Rev. C **86**, 064306 (2012).

[27] W. R. Zimmerman, M. W. Ahmed, B. Bromberger, S. C. Stave, A. Breskin, V. Dangendorf, Th. Delbar, M. Gai, S. S. Henshaw, J. M. Mueller, C. Sun, K. Tittelmeier, H. R. Weller, and Y. K. Wu, Phys. Rev. Lett. **110**, 152502 (2013).

[28] M. Freer, S. Almaraz-Calderon, A. Aprahamian, N. I. Ashwood, M. Barr, B. Bucher, P. Copp, M. Couder, N. Curtis, X. Fang, F. Jung, S. Lesher, W. Lu, J. D. Malcolm, A. Roberts, W. P. Tan, C. Wheldon, and V. A. Ziman, Phys. Rev. C **83**, 034314 (2011).

[29] P. H. C. Lau and N. S. Manton, Phys. Rev. Lett. **113**, 232503 (2014).

[30] C. Wheldon, T. Kokalova, M. Freer, A. Glenn, D. J. Parker, T. Roberts, and I. Walmsley, Phys. Rev. C **90**, 014319 (2014).

[31] J. H. Kelley, J. E. Purcell, and C. G. Sheu, Nucl. Phys. A **968**, 71 (2017).

[32] O. Tengblad, U. C. Bergmann, L. M. Fraile, H. O. U. Fynbo, and S. Walsh, Nucl. Instrum. Methods Phys. Res. A **525**, 458 (2004).

[33] D. Torresi, D. Stanko, A. Di Pietro, P. Figuera, M. G. Fisichella, M. Lattuada, M. Milin, A. Musumarra, M. Pellegriti, V. Scuderi, E. Strano, and M. Zadro, Nucl. Instrum. Methods Phys. Res. A **713**, 11 (2013).

[34] L. Grassi, J. Forneris, D. Torresi, L. Acosta, A. Di Pietro, P. Figuera, M. Fisichella, V. Grilj, M. Jakšić, M. Lattuada, T. Mijatović, M. Milin, L. Prepolec, N. Skukan, N. Soić, V. Tokić, and M. Uroić, Nucl. Instrum. Methods Phys. Res. A **767**, 99 (2014).

[35] M. Uroić, M. Milin, A. Di Pietro, P. Figuera, M. Fisichella, M. Lattuada, I. Martel, Đ. Miljanić, M. G. Pellegriti, L. Prepolec, A. M. Sánchez Benítez, V. Scuderi, N. Soić, E. Strano, and D. Torresi, Eur. Phys. J. **A 51**, 93 (2015).

[36] D. Jelavić Malenica, Ph.D. thesis, University of Zagreb, 2015 (unpublished).

[37] E. Costanzo, M. Lattuada, S. Romano, D. Vinciguerra, and M. Zadro, Nucl. Instrum. Methods Phys. Res. A **295**, 373 (1990).

[38] Y. N. Pavlenko, V. M. Pugach, V. A. Kiva, V. I. Medvedev, Y. O. Vasiliev, V. N. Dobrikov, and I. N. Kolomiets, Izv. Akad. Nauk Ser. Fiz. **57**, 140 (1993) [Bull. Rus. Acad. Sci. Phys. **57**, 1788 (1993)].

[39] M. Milin, M. Zadro, S. Cherubini, T. Davinson, A. Di Pietro, P. Figuera, Đ. Miljanić, A. Musumarra, A. Ninane, A. N. Ostrowski, M. G. Pellegriti, A. C. Shotter, N. Soić, and C. Spitaleri, Nucl. Phys. A **753**, 263 (2005).

[40] P. Papka, T. A. D. Brown, B. R. Fulton, D. L. Watson, S. P. Fox, D. Groombridge, M. Freer, N. M. Clarke, N. I. Ashwood, N. Curtis, V. Ziman, P. McEwan, S. Ahmed, W. N. Catford, D. Mahboub, C. N. Timis, T. D. Baldwin, and D. C. Weisser, Phys. Rev. C **75**, 045803 (2007).

[41] Tz. Kokalova, M. Freer, Z. Buthelezi, J. Carter, R. W. Fearick, S. V. Förtsch, H. Fujita, R. Neveling, P. Papka, F. D. Smit, J. A. Swartz, and I. Usman, Phys. Rev. C **87**, 057307 (2013).

[42] W. Buck, T. Rohwer, G. Staudt, A. Zimke, and F. Vogler, Nucl. Phys. A **297**, 231 (1978).

[43] C. Jacquot, Y. Sakamoto, M. Jung, and L. Girardin, Nucl. Phys. A **201**, 247 (1973).

[44] D. Miljanić, E. Kossionides, G. Vourvopoulos, and P. Assimakopoulos, Z. Phys. A **312**, 267 (1983).